European Radiology (2019) 29:3791–3801
https://doi.org/10.1007/s00330-019-06150-7

GASTROINTESTINAL

Iso- or hyperintensity of hepatocellular adenomas on hepatobiliary phase does not always correspond to hepatospecific contrast-agent uptake: importance for tumor subtyping

Edouard Reizine[1,2] · Maxime Ronot[2,3,4] · Frederic Pigneur[1] · Yvonne Purcell[2] · Sebastien Mulé[1] · Marco Dioguardi Burgio[2] · Julien Calderaro[5,6,7] · Giuliana Amaddeo[6,7,8] · Alexis Laurent[6,9] · Valérie Vilgrain[2,3,4] · Alain Luciani[1,6,7]

Received: 8 November 2018 / Revised: 21 February 2019 / Accepted: 8 March 2019 / Published online: 1 April 2019

Abstract

Purpose This study was conducted in order to evaluate if iso- or hyperintensity of HCAs on HBP is systematically related to a high uptake of hepatospecific contrast agent, using a quantitative approach.

Methods This bicentric retrospective study included all patients with histologically confirmed and subtyped HCA from 2009 to 2017 who underwent MRI with HBP after Gd-BOPTA injection and who showed iso- or hyperintensity on HBP. The signal intensity of tumors on pre- and postcontrast images and the presence of hepatic steatosis were noted. Contrast uptake on HBP was quantified using the liver-to-lesion contrast enhancement ratio (LLCER) and compared between HCA subtypes (Wilcoxon signed-rank test). Categorical variables were compared using chi-square tests.

Results Twenty-four HCAs showed iso- or hyperintensity on HBP, specifically 17 inflammatory (IHCAs) and 7 β-catenin HCAs (BHCAs). Eighteen HCAs (75%) (17 IHCAs and 1 BHCAs) had a LLCER < 0% (median − 13.6%, group 1), of which 94% were hyperintense on precontrast T1-W images, with background hepatic steatosis. Six HCAs (25%) had LLCER ≥ 0% (median 2.9%, group 2), and all were BHCAs. A LLCER ≥ 1.6% was associated with the diagnosis of BHCA with a sensitivity of 86% and a specificity of 100%.

Conclusion In conclusion, iso- or hyperintensity of hepatocellular adenomas on HBP does not necessarily correspond to an increased hepatospecific contrast-agent uptake. In IHCA, tumor hyperintensity on precontrast images and the underlying steatosis likely explain such iso- or hyperintensity, which do show reduced HBP contrast-agent uptake. On the other hand, marked contrast uptake can be observed, especially in BHCA.

Electronic supplementary material The online version of this article (https://doi.org/10.1007/s00330-019-06150-7) contains supplementary material, which is available to authorized users.

✉ Maxime Ronot
maxime.ronot@aphp.fr

[1] Department of Radiology, APHP, HU Henri Mondor, Creteil, Val-de-Marne, France

[2] Department of Radiology, APHP, University Hospitals Paris Nord Val de Seine, Beaujon, 100 Boulevard du Général Leclerc, 92118 Clichy, Hauts-de-Seine, France

[3] University Paris Diderot, Sorbonne Paris Cité, Paris, France

[4] INSERM U1149, centre de recherche biomédicale Bichat-Beaujon, CRB3, Paris, France

[5] Department of Pathology, APHP, HU Henri Mondor, Creteil, Val-de-Marne, France

[6] Faculté de Médecine, Universite Paris Est Creteil, 94010 Creteil, France

[7] INSERM Unit U 955, Equipe 18, 94010 Creteil, France

[8] Department of Hepatology, APHP, HU Henri Mondor, Creteil, Val-de-Marne, France

[9] Department of Liver Surgery, APHP, HU Henri Mondor, Creteil, Val-de-Marne, France

Key Points

- *Iso- or hyperintensity on HBP does not necessarily reflect a high uptake of hepatospecific contrast agent.*
- *Discrepancies between qualitative signal intensity and quantitative hepatospecific contrast uptake can be explained in IHCA by a combination of tumor hyperintensity on precontrast images and underlying hepatic steatosis.*
- *In BHCA, iso- or hyperintensity on HBP does actually correspond to a greater contrast uptake than that of the liver, demonstrated by an increased lesion-to-liver contrast enhancement ratio (LLCER).*

Keywords Adenoma · Liver neoplasms · Contrast media · Magnetic resonance imaging

Abbreviations

BHCA	β-Catenin-mutated hepatocellular adenoma
FNH	Focal nodular hyperplasia
HBP	Hepatobiliary phase
HCA	Hepatocellular adenoma
HHCA	HNF1-α-inactivated HCA
IHCA	Inflammatory HCA
LLCER	Liver-to-lesion contrast enhancement ratio
OATP	Organic anion transporting polypeptide
SI	Signal intensity
SIR	Signal intensity ratio

Introduction

Hepatocellular adenomas (HCAs) are rare benign hepatocellular tumors that mainly develop in young females taking oral contraception [1–5]. The two main complications are tumor hemorrhage and malignant transformation, which justifies liver resection in high-risk patients [4]. Recently, the European Association for the Study of the Liver issued recommendations for the management of HCA [4], acknowledging that the risk of complications is mostly influenced by tumor size and patient gender [6, 7]. Aside from that, subtyping of HCA should also be considered since different subtypes are associated with different outcomes [8]. Indeed, HNF1-α-inactivated HCA (HHCA) has a low potential for malignant transformation, which is not the case for β-catenin-mutated lesions (BHCAs) [8]. In addition, inflammatory IHCA has a high risk of tumor bleeding [5, 8].

MR imaging has been shown to be accurate for HCA subtyping, with combinations of features being associated with different tumor phenotypes [9–11]. In the two most common subtypes, HHCA and IHCA, the sensitivity and specificity of MRI have been reported to reach 90% [10–12]. Yet these results have been reported in studies using extracellular MR contrast agents [12].

After injection of hepatobiliary MR contrast agents [13–15], focal nodular hyperplasia (FNH) is characterized by iso- or hyperintensity on hepatobiliary phase (HBP), whereas HCA typically appears hypointense owing to the over- and reduced expression of organic anion transporting polypeptide (OATP) transporters, respectively [16–21]. Yet, several recent studies have reported HCAs showing iso- or hyperintensity on HBP in up to 26 to 67% of cases [22–24]. This has been described with both Gd-BOPTA (gadobenate dimeglumine, Multihance, Bracco Imaging) and Gd-EOB-DTPA (gadoxetic acid, Primovist, Bayer-Schering Pharma). In most series, such iso- or hyperintensity was depicted in IHCA [22–26]. Based on these results, a recent study even questioned the ability of MRI using hepatobiliary MR contrast agents to accurately distinguish FNH from HCAs [26]. Yet, this is in contradiction with the molecular background of IHCA, as their OATP expression has been shown to be lower than that of the adjacent liver [27, 28]. Hence, the iso- or hyperintensity reported in IHCA could be seen even in lesions showing potentially reduced contrast uptake on HBP. Conversely, molecular studies have shown that OATP expression is persistent in BHCA [28, 29], and imaging studies have reported BHCA showing iso- or hyperintensity on HBP, in accordance with their OATP expression [22, 28]. As a result, authors have attempted to overcome these shortcomings by trying to quantify the hepatospecific contrast uptake on HBP which could better match the molecular expression of these benign tumors.

Roux et al introduced the concept of lesion to liver contrast enhancement ratio (LLCER) as a quantitative tool for measuring Gd-BOPTA uptake within benign hepatocellular tumors [30]. The authors showed that LLCER improved the differentiation of FNH and HCA [30]. Yet, their approach has not been applied to refine the subtyping of HCA on HBP. In addition, the authors did not specifically address the issue of iso- or hyperintense HCAs on HBP.

Hence, the purpose of the current study was to evaluate if iso- or hyperintensity of HCAs on HBP is systematically related to a high uptake of hepatospecific contrast agent, using a quantitative analysis of the liver-to-lesion contrast enhancement ratio.

Materials and methods

Patient population

This retrospective study was approved by the local IRB and informed consent was waived. Between June 2009 and

September 2017, all patients with a pathologically proven hepatocellular adenoma were extracted from the databases of two imaging departments (Hospital Henri Mondor, Créteil, France: center 1 with 109 patients; and Hospital Beaujon, Clichy, France: center 2 with 93 patients). Out of 202 identified patients, a total of 59 patients underwent Gd-BOPTA-enhanced liver MRI with HBP acquisition (36 patients from center 1 and 23 patients from center 2) within 2 months prior to pathological analysis. Seventeen of these 59 patients (10 patients from center 1 and 7 patients from center 2), including 24 HCAs showing iso- or hyperintensity on HBP images, constituted the study population. The flowchart of the study population is presented in Fig. 1. Of the 24 included HCAs, data from 3 BHCAs have already been published in a previous manuscript focusing on a correlation between the quantitative analysis of benign hepatocellular tumor uptake on HBP imaging and the quantitative level of OATP expression [28]. Demographics and clinical and laboratory data were documented for all patients.

Pathological analysis

Diagnosis of all HCAs including subtyping was performed according to a combination of established morphological and immunophenotypical criteria by an expert pathologist (JC with 25 years of expertise in the field on liver tumors) [8, 31–33]. HCAs were defined as a proliferation of neoplastic hepatocytes with little or no atypia. The nontumoral liver was systematically analyzed. Steatosis was assessed visually, expressed in percentage form and graded according to the Brunt classification: mild (5–33%), moderate (34–66%), or severe (67–100%) [34].

Details of immunohistochemistry, diagnosis, and lesion classification are provided in the Electronic supplementary material.

MRI technique

MR imaging examinations were performed on a 1.5-T clinical MR scanner (Avanto, Siemens) in center 1 and 3.0 T MRI (Achieva, Philips Healthcare) in center 2.

Detailed MRI protocols can be found in Table 1 and in the Electronic supplementary material.

Qualitative analysis of HBP images

Enhancement on HBP images was initially assessed qualitatively by two radiologists independently (with respective 4 and 12 years' experience in abdominal MRI) based on analysis of HBP fat-suppressed 3D GRE T1-WI sequences analysis. Both radiologists were blinded to the final pathological diagnosis. A lesion was classified as being hypointense on HBP images when it showed homogeneous signal hypointensity relative to the adjacent liver parenchyma on the transverse slice showing the largest diameter of the lesion. Otherwise, the lesion was classified as iso- or hyperintense on HBP images and was available for quantitative analysis. In case of discrepancies, a consensus was reached with a third radiologist, with 15 years' experience in liver MRI.

For each patient, the presence of hepatic steatosis, defined by the visual analysis of signal dropout on opposed phase images, and the precontrast signal intensity of the lesion were noted [35].

Quantitative analysis

The quantitative analysis of contrast uptake on HBP was performed for each HCA during a separate reading 2 months after the qualitative reading session by the same two radiologists, blinded to the final pathological diagnosis and independently in order to assess interobserver agreement. In case of

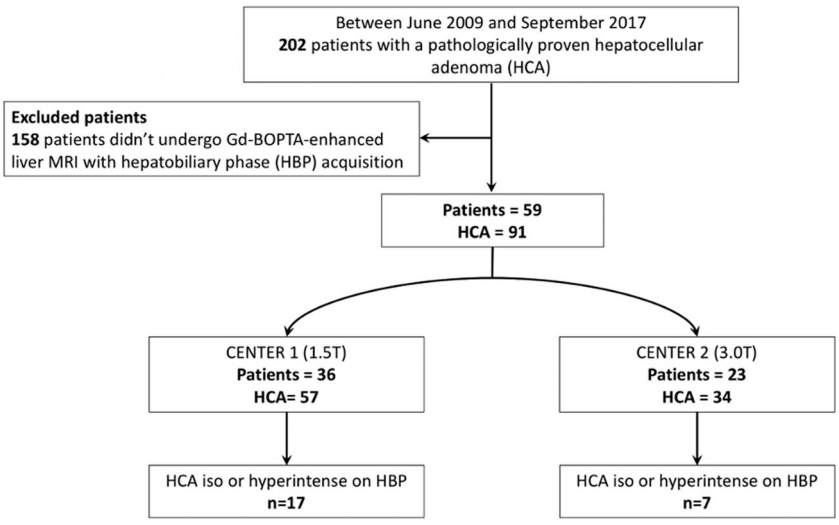

Fig. 1 Flowchart of the study

Table 1 MRI sequence parameters at 1.5 and 3 T

Sequences	Repetition time (ms)	Echo time (ms)	Flip angle (α)	Section thickness (mm)	Field of view (mm)	Bandwidth (Hz/px)
IP and OPT1 WI (center 1)	143	2.38–4.76	70	5	320	460
IP and OPT1 WI (center 2)	3.86	2.37	8	4	306	1430
FS-TSE-T2 WI (center 1)	1880	92	150	5	320	260
FS-TSE-T2 WI (center 2)	2000	120	90	5.50	331	271
Single-shot TSE T2-WI (center 1)	900	84	150	3	320	381
Single-shot TSE T2-WI (center 2)	471	120	90	4	302	599
DWI (center 1)	4700	52	90	6	128	1347
DWI (center 2)	1577	55	90	4.50	320	3417
3D-T1 FS GRE (center 1)	4,69	2.15	10	3	351	350
3D-T1 FS GRE (center 2)	3.21	0	10	5	322	1705

3D-T1 FS GRER were repeated with the same parameters for HBP

T1- or *T2-WI* = T1- or T2-weighted imaging, *GRE* = gradient recalled echo, *IP* = in phase, *OP* = out-of-phase, *TSE* = turbo spin echo, *FS* = fat-suppressed, *DWI* = diffusion-weighted imaging

discrepancies, a consensus was reached with a third radiologist, with 15 years' experience in liver MRI.

The radiologists computed the LLCER, following Roux et al [30]. Regions of interest (ROIs) were manually drawn in tumors and in the adjacent liver parenchyma on precontrast fat-suppressed T1-weighted images and on Gd-BOPTA-enhanced HBP images according to the following rules: (1) lesion ROIs were manually drawn to cover the entire surface of the lesion in the transverse plane that showed the largest diameter of the lesion. The contours of the ROI precisely matched those of each lesion, even in lesions with irregular borders. (2) A circular ROI was placed in the adjacent liver parenchyma on the same transverse plane selected for the liver lesion analysis and in the same anteroposterior position to avoid heterogeneities due to surface coils. The size of these ROIs was arbitrarily chosen between 100 and 200 mm^2, avoiding liver lesions or vessels (Supplementary Fig. 1).

For each HCA, the signal intensity ratio (SIR), defined as $SIR = 100 \times \frac{SI_{Tpost}}{SI_{LVpost}}$, and the LLCER, defined as $LLCER = 100 \times \frac{\left[\left(\frac{SI_{Tpost}}{SI_{LVpost}}\right) - \left(\frac{SI_{Tpre}}{SI_{LVpre}}\right)\right]}{\frac{SI_{Tpre}}{SI_{LVpre}}}$, were calculated, where SI_{Tpost} and SI_{LVpost} are the respective signal intensity (SI) of the tumor and liver on HBP sequences, and SI_{Tpre} and SI_{LVpre} are the respective SI of the tumor and liver before injection on the same pre- and postcontrast fat-suppressed 3D GRE T1-WI sequence.

The mean SIR and LLCER were measured for all lesions. As previously described [30], the SIR reflects the quantification of the relative signal intensity of the lesion as compared to that of the adjacent parenchyma. The LLCER reflects the relative contrast uptake of the lesion relative to that of the adjacent liver, irrespective of its SIR.

Lesions were further categorized into two distinct groups: group 1 for lesions with negative LLCER (< 0%, lower contrast uptake than the surrounding liver) and group 2 with positive LLCER (≥ 0%, i.e., similar or higher contrast uptake than the surrounding liver).

Statistical analysis

Categorical variables are presented as count and percentages, and continuous variables as means (standard deviations) or medians (ranges). A Kolmogorov–Smirnov test was used to assess the normality of our population. Comparison of categorical variables was performed using a McNemar test to take into consideration repeated measures. We used a binomial distribution-corrected version of the test to compensate for small effectives. Continuous data were compared using the Wilcoxon signed-rank test. Interobserver agreement was evaluated using intraclass correlation coefficient (ICC). The sensitivities and specificities of each ratio that allowed differentiation of HCA subtypes were determined with a receiver operating characteristic (ROC) curve analysis, using a nonparametric approach.

Tests were two-tailed, and p value of < 0.05 was considered statistically significant. All analyses were performed with SPSS (IBM Corp. Released 2013. IBM SPSS Statistics for Macintosh, Version 22.0) and R Core Team (2017, Version 1.1.442).

Results

Population

Mean age at inclusion was 35 ± 9 years (range 23–52). No patient had HBV or HCV infection. Two patients had two HCAs, one patient had three HCAs, and one patient had four

Table 2 Patient population

Patient	Center	Gender	Age	HBV- and HCV-positive serology	Steatosis (Brunt)	Number of lesion	Diagnostic confirmation	HCA subtype	Maximum lesion diameter (mm)	Precontrast signal intensity	HBP signal intensity	LLCER value (%)
1	1	F	23	0	0	2	Resection	β-Catenin-mutated HCA	111	Hypointense	Hyperintense	1.6
							Resection	β-Catenin-mutated HCA	57	Hypointense	Hyperintense	2.4
2	1	M	44	0	1 (mild)	1	Resection	β-Catenin-mutated HCA	15	Hyperintense	Hyperintense	2.9
3	1	M	25	0	0	1	Resection	β-Catenin-mutated HCA	71	Hyperintense	Hyperintense	7.6
4	1	M	26	0	0	1	Resection	β-Catenin-mutated HCA	104	Hypointense	Hyperintense	8.7
5	2	F	44	0	0	1	Biopsy	β-Catenin-mutated HCA	58	Hypointense	Hyperintense	20.6
6	1	F	50	0	1 (severe)	2	Biopsy	Inflammatory HCA	15	Hyperintense	Isointense	− 14.2
							Biopsy	Inflammatory HCA	25	Hyperintense	Isointense	− 7.8
7	1	F	36	0	1 (severe)	3	Biopsy	Inflammatory HCA	40	Hyperintense	Hyperintense	− 21.8
							Biopsy	Inflammatory HCA	32	Hyperintense	Hyperintense	− 11.4
							Biopsy	Inflammatory HCA	21	Hyperintense	Hyperintense	− 21.1
8	1	F	52	0	1 (mild)	1	Biopsy	Inflammatory HCA	28	Hyperintense	Isointense	− 10.1
9	2	F	26	0	1 (mild)	1	Resection	Inflammatory HCA	74	Hyperintense	Hyperintense	− 9.5
10	2	F	27	0	0	1	Resection	β-Catenin-mutated HCA	81	Hypointense	Hyperintense	− 13.1
11	2	F	44	0	1 (mild)	1	Resection	Inflammatory HCA	73	Hyperintense	Hyperintense	− 10.4
12	2	F	39	0	1 (moderate)	1	Biopsy	Inflammatory HCA	38	Hyperintense	Isointense	− 0.1
13	2	F	30	0	1 (severe)	1	Biopsy	Inflammatory HCA	52	Hyperintense	Hyperintense	− 28.9
14	2	F	34	0	1 (mild)	1	Biopsy	Inflammatory HCA	56	Hyperintense	Isointense	− 15.5
15	1	M	27	0	1 (moderate)	4	Resection	Inflammatory HCA	150	Hyperintense	Isointense	− 7.8
							Resection	Inflammatory HCA	87	Hyperintense	Isointense	− 18.6
							Resection	Inflammatory HCA	27	Hyperintense	Isointense	− 14.7
							Resection	Inflammatory HCA	44	Hyperintense	Hyperintense	− 11.6
16	1	F	29	0	1 (moderate)	1	Biopsy	Inflammatory HCA	14	Hyperintense	Isointense	− 21.8
17	1	F	40	0	1 (mild)	1	Biopsy	Inflammatory HCA	58	Hyperintense	Hyperintense	− 27.5

HCA = hepatocellular adenoma, *HBV* = hepatitis B virus, *HCV* = hepatitis C virus, *F* = female, *M* = male, *HBP* = hepatobiliary phase, *LLCER* = liver-to-lesion contrast enhancement ratio

HCAs. The mean size of all lesions was 55 ± 34 mm. Hepatic steatosis was present on pathological analysis in 12 patients, including 18 HCAs and 1 BHCA, and was graded accordingly as mild in 6 cases, moderate in 3 cases, and severe in 3 cases. The final diagnosis of HCA was made on the basis of pathological analysis postliver resection ($n = 12$) and liver biopsy ($n = 12$) and identified 17 IHCAs and 7 BHCAs.

Patients' clinical, biological, and pathological findings are provided in Table 2.

Qualitative analysis of liver MRI

Details of the qualitative analysis of liver MRI are provided in Table 3.

Hepatic steatosis was identified in 12 patients, with perfect agreement with pathological findings.

- Inflammatory HCA: Fifteen IHCAs (15/17) appeared isointense on HBP and two appeared hyperintense (Fig. 2). All IHCAs were developed on an underlying hepatic steatosis and showed high-signal intensity on precontrast T1-weighted sequences.
- β-Catenin-mutated HCA: All BHCAs appeared hyperintense on HBP (Fig. 3). Only one of seven BHCAs was identified in a liver with underlying steatosis. This BHCA showed high signal intensity on precontrast T1-W sequences. The remaining six BHCAs were not associated with hepatic steatosis: five of these BHCAs appeared isointense, and one appeared hyperintense on precontrast T1-W sequences.

Quantitative analysis of Gd-BOPTA uptake

Details of the quantitative analysis are provided in Table 4.

The ICC for interobserver agreement was 0.78 (95% CI 0.44–0.93) for LLCER and 0.30 (95% CI 0.32–0.7) for SIR measurements.

The mean LLCER of the 24 lesions was − 9.3 ± 12.1%, with a median of − 10.9%. The mean and median SIR of the 24 lesions were 103.0 ± 16.2 and 102.0%.

Eighteen tumors (72%) belonged to group 1 (LLCER < 0%) with a median LLCER of − 13.6% (range − 28.9, −0.1%). This group included the 17 IHCAs and 1 BHCA.

Six lesions (28%) belonged to group 2 (LLCER ≥ 0%) with a median LLCER of 5.3% (range 1.6, 20.6%). All tumors in this group were BHCA. The LLCER value in group 1 was significantly lower than that in group 2, $p < 0.001$. Seventeen lesions in group 1 (94%) were associated with hepatic steatosis, as opposed to one in group 2 (17%) (Fig. 4).

Focusing on HCA subtypes, all IHCAs had a negative LLCER (median −14.2% (range −28.9, − 0.1%)), whereas six out of seven (86%) BHCAs had a positive LLCER (median 2.9% (range − 13.0, 20.6%)). The LLCER of BHCA was significantly higher than that of IHCA ($p < 0.001$). No significant difference was found between the SIR of BHCA and IHCA (medians 102.4 vs 101.0%, $p = 1.00$). A LLCER ≥ 1.6% was associated with the diagnosis of BHCA with a sensitivity of 86% and a specificity of 100% (Fig. 5).

Discussion

The purpose of the current study was to evaluate if iso-or hyperintensity of HCAs on HBP was systematically related to a high uptake of hepatospecific contrast agent. Based on the quantitative analysis of the liver-to-lesion contrast enhancement ratio, our findings first suggest that iso- or hyperintensity of HCAs on HBP is not necessarily triggered by hepatospecific contrast uptake and may rather be explained by the combination of spontaneous tumor hyperintensity on precontrast T1-weighted images and underlying steatosis. Secondly, our results also suggest that in normal livers—i.e., without underlying liver steatosis—hyperintensity on HBP is related to true contrast-agent uptake and can correspond to BHCA.

Thirty-four percent of IHCAs were iso- or hyperintense on HBP in the current study. This is within the range of reported rates, slightly higher than the results from Ba-Ssalamah et al

Table 3 Qualitative MR imaging features of benign hepatocellular tumors

	Inflammatory HCA	β-Catenin-mutated HCA	*p* value
Number of lesions	17	7	
Maximum lesion diameter (mm) (mean ± SD)	49.1 ± 33.7	71 ± 32.4	0.100*
High-signal intensity on precontrast 3D GRE T1-WI	17 (100)	2 (29)	0.017**
Hepatic steatosis	17 (100)	1 (14)	0.035**

Data are the number of lesions, and data in parentheses are the percentage

HCA = hepatocellular adenoma, *T1-WI* = T1-weighted imaging, *GRE* = gradient recalled echo

*Wilcoxon signed-rank test

**Adjusted McNemar test with binomial distribution

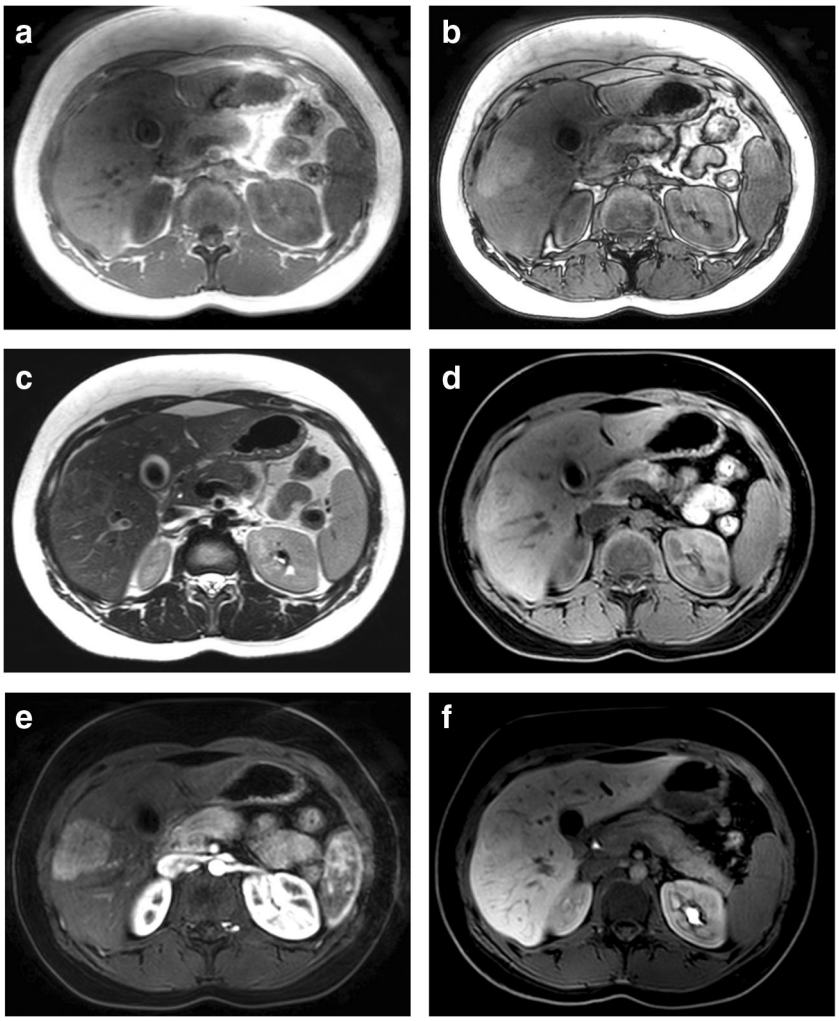

Fig. 2 A 31-year-old female patient referred for the diagnosis of a 5-cm liver nodule. Liver MRI shows underlying hepatic steatosis (**a** + **b**). The lesion shows peripheral hyperintensity on the T2-weighted sequence (**c**), hyperintensity on precontrast T1-weighted fat-saturated images (**d**), homogeneous hyperintensity on the arterial phase (**e**), and appears heterogeneously hyperintense on HBP (**f**). The liver-to-lesion contrast enhancement ratio (LLCER) was measured at − 29%. The final diagnosis was inflammatory hepatocellular adenoma (IHCA)

(29%) or Glockner et al (26%), but lower than Agarwal et al (46%) or Thomeer et al (67%) [22–24, 26]. All IHCAs showing iso- or hyperintensity on HBP developed in fatty livers and showed signal hyperintensity on precontrast T1-weighted images. Both features have been shown to be frequent in the setting of IHCA [10, 36]. Yet, all IHCAs had a negative LLCER on quantitative analysis in line with molecular studies showing that IHCAs have a decreased expression of OATP [22, 27, 28]. We believe that these results explain the discrepancy between the qualitative and quantitative analyses on HBP. Indeed, the higher signal intensity of the liver on HBP is counterbalanced by the signal intensity decrease induced by saturation of fat signal and by the precontrast high intensity of the lesion. Even if this cannot be retrospectively demonstrated, we strongly believe that most IHCAs reported as iso- or hyperintense on HBP in previous publications fall into this category [24].

Interestingly, in the absence of steatosis, iso- or hyperintensity on HBP was significantly associated with the diagnosis of BHCA, and 86% of them had a positive LLCER, reflecting a higher tumor contrast uptake on HBP when compared to the liver. This is also in line with molecular studies showing that OATP expression is conserved in BHCA [27–29]. OATP expression has been shown to be strongly associated with the expression of Wnt/β-catenin target genes [29, 37]. To our knowledge, there is to date no imaging feature associated with the presence of β-catenin mutation. The authors have reported that a faint scar may be a possible sign of BHCA, but the number of published cases remains very low, and this feature does not seem to have high specificity [36, 38]. If validated in larger patient populations, the current results might be of utmost clinical value given the need for assessment of the presence of β-catenin mutation [4, 5].

The current study reinforces the importance of quantitative analysis of contrast uptake on HBP, particularly in the case of underlying steatosis. Interestingly, the SIR, which reflects the qualitative interpretation of the relative signal intensity of a lesion compared to that of the adjacent liver on HBP, did not allow a correct distinction between IHCA and BHCA. Hence, quantitative analysis should reflect the actual uptake of contrast agent, and not the relative signal intensity of a lesion versus the liver. To date, such analysis using the LLCER has

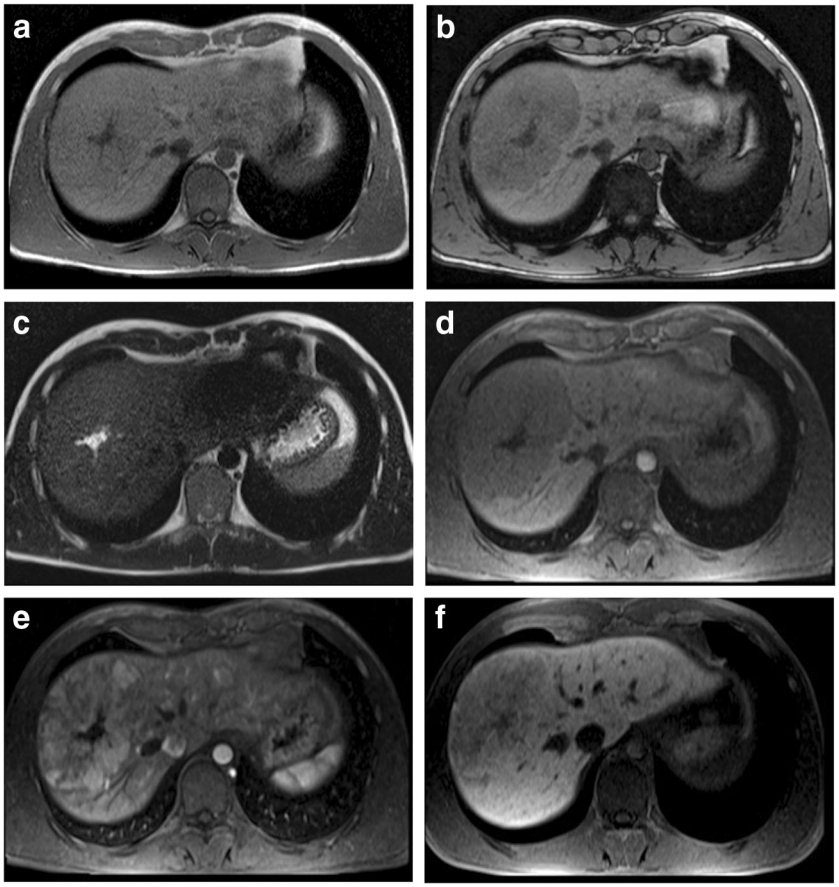

Fig. 3 A 34-year-old male referred for the diagnosis of a large right lobe of liver mass. Liver MRI shows on a nonsteatotic underlying liver (**a** + **b**). The lesion shows iso-intensity on the T2-weighted sequence with a central hyperintense area (**c**), hypointensity on precontrast T1-weighted fat-saturated images (**d**), heterogeneous hyperintensity on the arterial phase (**e**), and appears heterogeneously hyperintense on HBP (**f**), consistent with hepatobiliary phase uptake. The liver-to-lesion contrast enhancement ratio (LLCER) was 8.7%. The final diagnosis was β-catenin-mutated hepatocellular adenoma (BHCA)

been limited to the differentiation of FNH from HCA with excellent sensitivity and specificity and has high interobserver correlation [30]. A recent letter suggested that the performance of LLCER might be improved by taking into account only those regions of maximum enhancement [39]. Yet, this may result in interreader variability in selecting the regions of highest intensity, particularly in this setting of heterogeneous uptake [40]. This explains the reason for selecting ROIs encompassing the entire tumor. The ROI drawn in the adjacent liver parenchyma should be placed on the same transverse plane selected for the liver lesion analysis and in the same anteroposterior position to avoid heterogeneities due to surface coils. We acknowledge that these issues further demonstrate the difficulty of quantitative analysis in routine clinical practice. However, the results of our current study suggest that the impact of quantitative analysis is limited in cases without underlying steatosis, for which hyperintensity on HBP seems to be truly related to hepatospecific contrast uptake. Importantly, in this situation, arterially enhanced lesions should be analyzed with caution as these could correspond to BHCA and not always to FNH.

Besides its retrospective design, this study suffers from several limitations. First, the magnetic field varied between the two centers. Interestingly, the proportions of iso–hyperintense HCAs were similar (30% in center 1, 21% in center 2), suggesting that the magnetic field does not affect

Table 4 Quantitative analysis of Gd-BOPTA uptake on hepatobiliary phase

	Group 1 LLCER < 0%	Group 2 LLCER ≥ 0%	*p* value
Number of lesions	18	6	
HCA subtypes	17 inflammatory HCA 1 β-catenin-mutated HCA	6 β-catenin-mutated HCA	0.035*
Median LLCER (ranges)	− 13.6% (− 28.9 to − 0.1%)	5.3% (1.6–20.6%)	< 0.001**

HCA = hepatocellular adenoma, *LLCER* = liver-to-lesion contrast enhancement ratio

*Adjusted McNemar test with binomial distribution

**Wilcoxon signed-rank test

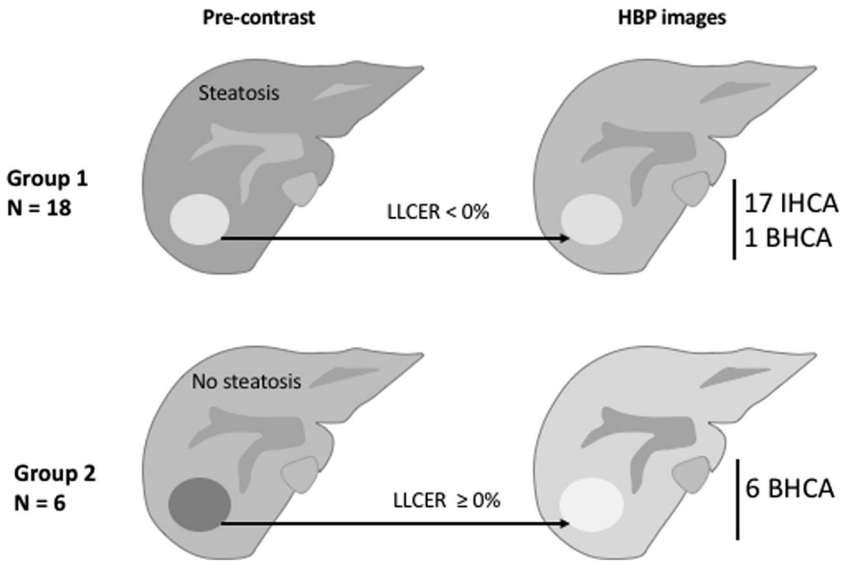

Fig. 4 Illustration of the different scenarios explaining iso- or hyperintensity of hepatocellular adenomas (HCAs) on hepatobiliary phase images. In group 1, iso- or hyperintensity is explained by the combination of hyperintensity on precontrast T1-weighted and hepatic steatosis, while the liver-to-lesion contrast enhancement ratio (LLCER) is negative. In group 2, the LLCER is positive, indicating higher uptake by the HCA when compared to the surrounding liver

the visual interpretation of hepatobiliary phase in HCA. A previous study showed that the quantitative indices of hepatic enhancement on hepatobiliary phase obtained using 1.5 and 3.0 T scanners were similar using Gd-EOB-DTPA [41]. To date, no study has focused on this using Gd-BOPTA, but the relaxivities of Gd-BOPTA and Gd-EOB-DTPA seem to vary similarly between 1.5 and 3 T [42]. Lastly, all quantitative analyses focused on relative tumor-to-liver signal intensity rather than on tumor signal intensity per se. Hence, the impact of field strengths appears limited. Second, the number of included patients is limited. Yet, this equates to a relatively large cohort, considering the prevalence of HCAs and the stringency of inclusion criteria. To date, our population of BHCA remains one of the most important published series. Third, the quantitative analysis was two-dimensional, which did not allow for an overall uptake evaluation. Yet, pathological and IHC analyses of tumors follow the same rules, with potential sample bias. Then, most studies analyzing benign hepatocellular tumors on HBP use Gd-EOB-DTPA. However, aside from the amount of contrast uptaken by hepatocytes, no difference has been reported regarding molecular mechanisms for contrast uptake between EOB and BOPTA [43]. Lastly, no cases of β-catenin-mutated IHCA were included, so it remains unclear whether LLCER may be useful in

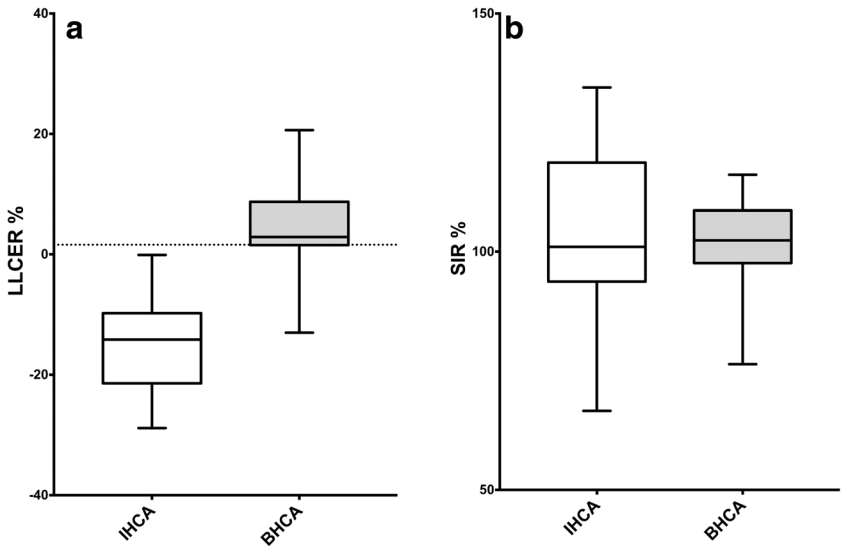

Fig. 5 Boxplots of liver-to-lesion contrast enhancement ratio (LLCER) (**a**) and the signal intensity ratio (SIR) (**b**) values in inflammatory hepatocellular adenoma (IHCA) and β-catenin-mutated hepatocellular adenoma (BHCA). The LLCER of BHCA was significantly higher than that of IHCA using Wilcoxon signed-rank test ($p < 0.001$). The median value is shown as a line across each box. Boxes stretch across the interquartile range, from lower quartile to upper quartile. Whiskers show the smallest observation and the largest observation (range of values). The line across both boxplots corresponds to a LLCER value of 1.6. A LLCER ≥ 1.6% was associated with the diagnosis of BHCA with a sensitivity of 86% and a specificity of 100%

subtyping these tumors. Finally, this study only focused on HCA. Therefore, the suggested LLCER thresholds only apply in known HCA and could not be used to differentiate HCA from FNH.

In conclusion, iso- or hyperintensity of hepatocellular adenomas on HBP does not necessarily correspond to an increased hepatospecific contrast-agent uptake. In IHCA, tumor hyperintensity on precontrast images and underlying steatosis likely explain such iso- or hyperintensity, which do show reduced HBP contrast-agent uptake. On the other hand, marked contrast uptake can be observed, especially in BHCA.

Funding The authors state that this work has not received any funding.

Compliance with ethical standards

Guarantor The scientific guarantor of this publication is Maxime Ronot.

Conflict of interest The authors declare that they have no conflict of interest.

Statistics and biometry No complex statistical methods were necessary for this paper.

Informed consent Written informed consent was waived by the Institutional Review Board.

Ethical approval Institutional Review Board approval was obtained.

Study subjects or cohorts overlap Some study subjects or cohorts have been previously reported in a previous manuscript in the *European Radiology* focusing on a correlation between the quantitative analysis of benign hepatocellular tumor uptake on HBP imaging and the quantitative level of OATP expression [28].

Methodology
- retrospective
- diagnostic or prognostic study
- multicenter study

References

1. Edmondson HA, Henderson B, Benton B (1976) Liver-cell adenomas associated with use of oral contraceptives. N Engl J Med 294: 470–472. https://doi.org/10.1056/NEJM197602262940904
2. Nault JC, Bioulac-Sage P, Zucman-Rossi J (2013) Hepatocellular benign tumors—from molecular classification to personalized clinical care. Gastroenterology 144:888–902. https://doi.org/10.1053/j.gastro.2013.02.032
3. Belghiti J, Cauchy F, Paradis V, Vilgrain V (2014) Diagnosis and management of solid benign liver lesions. Nat Rev Gastroenterol Hepatol 11:737–749. https://doi.org/10.1038/nrgastro.2014.151
4. European Association for the Study of the Liver (EASL) (2016) EASL clinical practice guidelines on the management of benign liver tumours. J Hepatol 65:386–398. https://doi.org/10.1016/j.jhep.2016.04.001
5. Nault JC, Paradis V, Cherqui D, Vilgrain V, Zucman-Rossi J (2017) Molecular classification of hepatocellular adenoma in clinical practice. J Hepatol 67:1074–1083. https://doi.org/10.1016/j.jhep.2017.07.009
6. Dokmak S, Paradis V, Vilgrain V et al (2009) A single-center surgical experience of 122 patients with single and multiple hepatocellular adenomas. Gastroenterology 137:1698–1705. https://doi.org/10.1053/j.gastro.2009.07.061
7. Farges O, Ferreira N, Dokmak S, Belghiti J, Bedossa P, Paradis V (2011) Changing trends in malignant transformation of hepatocellular adenoma. Gut 60:85–89. https://doi.org/10.1136/gut.2010.222109
8. Nault JC, Couchy G, Balabaud C et al (2017) Molecular classification of hepatocellular adenoma associates with risk factors, bleeding, and malignant transformation. Gastroenterology 152:880–894.e6. https://doi.org/10.1053/j.gastro.2016.11.042
9. Lewin M, Handra-Luca A, Arrivé L et al (2006) Liver adenomatosis: classification of MR imaging features and comparison with pathologic findings. Radiology 241:433–440. https://doi.org/10.1148/radiol.2412051243
10. Laumonier H, Bioulac-Sage P, Laurent C, Zucman-Rossi J, Balabaud C, Trillaud H (2008) Hepatocellular adenomas: magnetic resonance imaging features as a function of molecular pathological classification. Hepatology 48:808–818. https://doi.org/10.1002/hep.22417
11. Ronot M, Bahrami S, Calderaro J et al (2011) Hepatocellular adenomas: accuracy of magnetic resonance imaging and liver biopsy in subtype classification. Hepatology 53:1182–1191. https://doi.org/10.1002/hep.24147
12. Ronot M, Vilgrain V (2014) Imaging of benign hepatocellular lesions: current concepts and recent updates. Clin Res Hepatol Gastroenterol 38:681–688. https://doi.org/10.1016/j.clinre.2014.01.014
13. Kreft BP, Baba Y, Tanimoto A, Finn JP, Stark DD (1993) Orally administered manganese chloride: enhanced detection of hepatic tumors in rats. Radiology 186:543–548. https://doi.org/10.1148/radiology.186.2.8421762
14. Ni Y, Marchal G, Yu J, Mühler A, Lukito G, Baert AL (1994) Prolonged positive contrast enhancement with Gd-EOB-DTPA in experimental liver tumors: potential value in tissue characterization. J Magn Reson Imaging 4:355–363
15. Ni Y, Marchal G (1998) Enhanced magnetic resonance imaging for tissue characterization of liver abnormalities with hepatobiliary contrast agents: an overview of preclinical animal experiments. Top Magn Reson Imaging 9:183–195
16. Grazioli L, Morana G, Kirchin MA, Schneider G (2005) Accurate differentiation of focal nodular hyperplasia from hepatic adenoma at gadobenate dimeglumine-enhanced MR imaging: prospective study. Radiology 236:166–177. https://doi.org/10.1148/radiol.2361040338
17. Grazioli L, Bondioni MP, Haradome H et al (2012) Hepatocellular adenoma and focal nodular hyperplasia: value of gadoxetic acid-enhanced MR imaging in differential diagnosis. Radiology 262: 520–529. https://doi.org/10.1148/radiol.11101742
18. Bieze M, van den Esschert JW, Nio CY et al (2012) Diagnostic accuracy of MRI in differentiating hepatocellular adenoma from focal nodular hyperplasia: prospective study of the additional value of gadoxetate disodium. AJR Am J Roentgenol 199:26–34. https://doi.org/10.2214/AJR.11.7750
19. Suh CH, Kim KW, Kim GY, Shin YM, Kim PN, Park SH (2015) The diagnostic value of Gd-EOB-DTPA-MRI for the diagnosis of focal nodular hyperplasia: a systematic review and meta-analysis. Eur Radiol 25:950–960. https://doi.org/10.1007/s00330-014-3499-9
20. Neri E, Bali MA, Ba-Ssalamah A et al (2016) ESGAR consensus statement on liver MR imaging and clinical use of liver-specific

contrast agents. Eur Radiol 26:921–931. https://doi.org/10.1007/s00330-015-3900-3
21. Merkle EM, Zech CJ, Bartolozzi C et al (2016) Consensus report from the 7th international forum for liver magnetic resonance imaging. Eur Radiol 26:674–682. https://doi.org/10.1007/s00330-015-3873-2
22. Ba-Ssalamah A, Antunes C, Feier D et al (2015) Morphologic and molecular features of hepatocellular adenoma with gadoxetic acid-enhanced MR imaging. Radiology 277:104–113. https://doi.org/10.1148/radiol.2015142366
23. Agarwal S, Fuentes-Orrego JM, Arnason T et al (2014) Inflammatory hepatocellular adenomas can mimic focal nodular hyperplasia on gadoxetic acid-enhanced MRI. AJR Am J Roentgenol 203:W408–W414. https://doi.org/10.2214/AJR.13.12251
24. Thomeer MG, Willemssen FE, Biermann KK et al (2014) MRI features of inflammatory hepatocellular adenomas on hepatocyte phase imaging with liver-specific contrast agents. J Magn Reson Imaging 39:1259–1264. https://doi.org/10.1002/jmri.24281
25. Tse JR, Naini BV, Lu DSK, Raman SS (2016) Qualitative and quantitative gadoxetic acid-enhanced MR imaging helps subtype hepatocellular adenomas. Radiology 279:118–127. https://doi.org/10.1148/radiol.2015142449
26. Glockner JF, Lee CU, Mounajjed T (2017) Inflammatory hepatic adenomas: characterization with hepatobiliary MRI contrast agents. Magn Reson Imaging 47:103–110. https://doi.org/10.1016/j.mri.2017.12.006
27. Yoneda N, Matsui O, Kitao A et al (2016) Benign hepatocellular nodules: hepatobiliary phase of gadoxetic acid-enhanced MR imaging based on molecular background. Radiographics 36:2010–2027. https://doi.org/10.1148/rg.2016160037
28. Reizine E, Amaddeo G, Pigneur F et al (2018) Quantitative correlation between uptake of Gd-BOPTA on hepatobiliary phase and tumor molecular features in patients with benign hepatocellular lesions. Eur Radiol. https://doi.org/10.1007/s00330-018-5438-7
29. Yoneda N, Matsui O, Kitao A et al (2012) Beta-catenin-activated hepatocellular adenoma showing hyperintensity on hepatobiliary-phase gadoxetic-enhanced magnetic resonance imaging and overexpression of OATP8. Jpn J Radiol 30:777–782. https://doi.org/10.1007/s11604-012-0115-2
30. Roux M, Pigneur F, Calderaro J et al (2015) Differentiation of focal nodular hyperplasia from hepatocellular adenoma: role of the quantitative analysis of gadobenate dimeglumine-enhanced hepatobiliary phase MRI. J Magn Reson Imaging 42:1249–1258. https://doi.org/10.1002/jmri.24897
31. Fléjou JF (2011) WHO classification of digestive tumors: the fourth edition. Ann Pathol 31:S27–S31. https://doi.org/10.1016/j.annpat.2011.08.001
32. Zucman-Rossi J, Jeannot E, Nhieu JT et al (2006) Genotype-phenotype correlation in hepatocellular adenoma: new classification and relationship with HCC. Hepatology 43:515–524. https://doi.org/10.1002/hep.21068
33. Bioulac-Sage P, Laumonier H, Couchy G et al (2009) Hepatocellular adenoma management and phenotypic classification: the Bordeaux experience. Hepatology 50:481–489. https://doi.org/10.1002/hep.22995
34. Brunt EM, Janney CG, Di Bisceglie AM, Neuschwander-Tetri BA, Bacon BR (1999) Nonalcoholic steatohepatitis: a proposal for grading and staging the histological lesions. Am J Gastroenterol 94:2467–2474. https://doi.org/10.1111/j.1572-0241.1999.01377.x
35. Cassidy FH, Yokoo T, Aganovic L et al (2009) Fatty liver disease: MR imaging techniques for the detection and quantification of liver steatosis. Radiographics 29:231–260. https://doi.org/10.1148/rg.291075123
36. van Aalten SM, Thomeer MGJ, Terkivatan T et al (2011) Hepatocellular adenomas: correlation of MR imaging findings with pathologic subtype classification. Radiology 261:172–181. https://doi.org/10.1148/radiol.11110023
37. Ueno A, Masugi Y, Yamazaki K et al (2014) OATP1B3 expression is strongly associated with Wnt/β-catenin signalling and represents the transporter of gadoxetic acid in hepatocellular carcinoma. J Hepatol 61:1080–1087. https://doi.org/10.1016/j.jhep.2014.06.008
38. Thomeer MG, E Bröker ME, de Lussanet Q et al (2014) Genotype-phenotype correlations in hepatocellular adenoma: an update of MRI findings. Diagn Interv Radiol 20:193–199. https://doi.org/10.5152/dir.2013.13315
39. Thomeer MG, Gest B, van Beek H et al (2018) Quantitative analysis of hepatocellular adenoma and focal nodular hyperplasia in the hepatobiliary phase: external validation of LLCER method using gadobenate dimeglumine as contrast agent. J Magn Reson Imaging 47:860–861. https://doi.org/10.1002/jmri.25789
40. Roux M, Pigneur F, Luciani A (2018) Response to "Quantitative analysis of hepatocellular adenoma and focal nodular hyperplasia in the hepatobiliary phase: external validation of llcer method using gadobenate dimeglumine as contrast agent". J Magn Reson Imaging 47:862–863. https://doi.org/10.1002/jmri.25788
41. Hata H, Inoue Y, Nakajima A, Komi S, Miyatake H (2017) Influence of the magnetic field strength on image contrast in Gd-EOB-DTPA-enhanced MR imaging: comparison between 1.5T and 3.0T. Magn Reson Med Sci 16:109–114. https://doi.org/10.2463/mrms.mp.2015-0158
42. Rohrer M, Bauer H, Mintorovitch J, Requardt M, Weinmann HJ (2005) Comparison of magnetic properties of MRI contrast media solutions at different magnetic field strengths. Invest Radiol 40:715–724
43. Pascolo L, Cupelli F, Anelli PL et al (1999) Molecular mechanisms for the hepatic uptake of magnetic resonance imaging contrast agents. Biochem Biophys Res Commun 257:746–752. https://doi.org/10.1006/bbrc.1999.0454